CLASSIFICATION CHANGED TO

FILE COPY NO.

Copy No. RM No. L7D03

JAN 151952

# RESEARCH MEMORANDUM

CLASSIFICATION CHANGED TO UNCLASSIFIED AUTHORITY CROWLEY CHANGE #2110 12-14-53

AN INVESTIGATION OF THE LOW-SPEED CHARACTERISTICS OF

TWO SHARP-EDGE SUPERSONIC INLETS DESIGNED FOR

ESSENTIALLY EXTERNAL SUPERSONIC COMPRESSION

By

JIHIS DOCUMENT ON LOAN FROM THE FILES OF

John S. Dennard

Langley Memorial Aeronautical Laboratory NATIONAL ADVISORY COMMITTEE FOR AERONAUTICS Langley Field, Va. LANGLEY AEROMAUTICAL LABORATORY LANGLEY FIELD, HAMPTON, VIRGINIA

RETURN TO THE ABOVE ADDRESS.

REQUESTS FOR PUBLICATIONS SHOULD BE ADDRESSED AS FOLLOWS:

NATIONAL ADVISORY COMMITTEE FOR AERONAUTICS 1512 H STREET, N. W. WASHINGTON 25, D. C.

NATIONAL ADVISORY COMMITTEE FOR AERONAUTICS

WASHINGTON

June 6 1947

RESTRICTED
CONFIDENTIALY INFORMATION

NACA RM No. L7D03

NATIONAL ADVISORY COMMITTEE FOR AERONAUTICS

#### RESEARCH MEMORANDUM

AN INVESTIGATION OF THE LOW-SPEED CHARACTERISTICS OF

TWO SHARP-EDGE SUPERSONIC INLETS DESIGNED FOR

ESSENTIALLY EXTERNAL SUPERSONIC COMPRESSION

By John S. Dennard

# 

An investigation of two sharp-edge annular inlets with conical central bodies has been conducted at low airspeeds in the Langley propeller-research tunnel to obtain preliminary information concerning the surface-pressure, drag, and pressure-recovery characteristics of such inlets in the subsonic flight regime. Inlet A, which was designed for supersonic flight Mach numbers between 1.0 and 1.2, was essentially similar to the NACA transonic air inlet described in NACA Research Memorandums Nos. L6J04 and L7A06 except that it had a sharp-edge inlet lip. Inlet B, which was designed for supersonic flight Mach numbers up to about 3.0, was representative of the inlets described in NACA Research Memorandum No. L6J31. Surface-pressure measurements and surveys of the pressures in the internal and external flow were obtained at angles of attack of 0° and 6° for a wide range of inlet-velocity ratio.

It appears that the sharp-edge lips of such inlets will operate without serious pressure peaks only over a narrow range of inlet-velocity ratio. Flow separation from such cowling lips occurs outside of this range, on the external surface at lower inlet-velocity ratios and on the internal surface at higher inlet-velocity ratios. This separation is at first largely confined to a "bubble" near the leading edge which does not initiate large total-pressure losses over a fairly wide range of inlet-velocity ratio.

Internal losses for both inlets tested were of the same order as those for the previously tested NACA transonic inlet below an inlet-velocity ratio of 1.2. At inlet-velocity ratios above this value, the pressure recoveries were lower than that for the NACA transonic inlet. Similarly, it is indicated that the external drag for inlets A and B will be higher than that for the NACA transonic inlet, especially at low values of inlet-velocity ratio.

The external lip surface for such inlets can be designed for a desired critical Mach number (subsonic) through the use of existing data for the NACA 1-series nose inlets.

#### INTRODUCTION

In reference 1 a sharp-edge supersonic nose inlet is described in which the conical shock from the extended conical central body is utilized to obtain external supersonic compression and reduced flow velocities in the vicinity of the inlet. It appears that such an inlet will afford high pressure recoveries and smooth operating characteristics over a wide range of supersonic flight Mach numbers and can be designed for a drag only slightly greater than that for an inlet with completely internal supersonic compression. Because of the great interest in the subject inlets, the present investigation has been conducted in the Langley propeller-research tunnel to obtain preliminary information concerning the surface-pressure, drag, and pressure-recovery characteristics in the subsonic flight regime where the sharp inlet lips might cause serious separation effects.

The two test inlets were designed in accordance with the data contained in reference 1. Inlet A, which was designed for flight Mach numbers up to 1.2, was essentially similar to the NACA transonic air inlet except for the conventional round-edge lips of the transonic inlet. (See references 2 and 3.) However, as sharp-edge inlets have been proposed frequently for this flight regime, tests of this configuration were made to obtain data for a preliminary comparison of the two types of lip shapes.

Inlet B, which was designed for supersonic flight Mach numbers up to 3.0, is representative of the inlets reported in reference 1.

Surface pressures were measured over the top parts of the nose cone, inner and outer walls of the diffuser, and external cowling surface. Pressure surveys were made in the inlets and in the diffusers of both cowlings. Boundary-layer total-pressure surveys were made at the rear of the external cowling surfaces.

#### SYMBOLS

H total pressure, pounds per square foot

Hav average total pressure, pounds per square foot

Mcr	predicted critical Mach number
p	static pressure, pounds per square foot
Po	free-stream static pressure, pounds per square foot
q <sub>o</sub>	free-stream dynamic pressure, pounds per square foot
vi	average velocity of flow at inlet, feet per second
vo	free-stream velocity, feet per second
α	angle of attack, degrees
8 Selleto	boundary-layer thickness (defined as distance from surface to point where $\frac{H - p_0}{q_0} = 0.95$ ), inches

## MODEL AND TESTS

Line drawings of the two inlets tested are presented as figure 1. It is noted that the shapes of the diffusers and cowlings for the two inlets were necessarily dissimilar due to the differences in nose angle, cowling position, and inlet-lip angle. The transition between the nose and diffuser surface of inlet A was a bend of small radius as contrasted to the long smooth transition for inlet B. A simple radius was used in inlet A to fair between the wedge-shape lip section and the maximum thickness of the test body; a portion of the external shape for an NACA 1-77.5-050 nose inlet (reference 4) was used for the corresponding transition fairing for inlet B. (See detail, fig. 1.) Inlet areas were 1.106 square feet for inlet A and 0.695 square foot for inlet B. Inlet A used the same conical nose and had approximately the same inlet area as the NACA annular transonic air inlet tested in reference 2.

The general arrangement and over-all dimensions of the model are presented as figure 2, and photographs of the model with the two inlets installed are shown as figures 3 through 6. The internal-flow system included a 25-horsepower axial-flow fan, which was necessary to obtain the higher inlet-velocity ratios. Control of the flow quantity was obtained by varying the rotational speed of the fan and the position of the butterfly-type shutters. Internal-flow quantities were measured by means of the total- and static-pressure

tubes at the throat of the venturi and checked by a rake at the exit. A thermocouple attached to the exit rake was used to measure the temperature rise through the fan.

Prior to the tunnel tests, the venturi in the tail of the model was calibrated to assure the accuracy of the internal flow quantity measurements. It was found that accurate measurements could be obtained so long as the fan did not introduce appreciable rotation in the flow through the throat of the venturi. It was also determined that such rotation could be avoided for any desired flow quantity by simultaneous adjustment of the fan rotational speed and the position of the flow-control shutters. During the tunnel tests, the existence of a uniform static-pressure distribution in the venturi throat, which was indicative of the avoidance of flow rotation, was established for each test condition by visual observations of a multitube manometer.

Surface pressures were measured by means of 52 orifices installed at the tops of the noses, diffuser surfaces, and external cowling surfaces. Inlet pressure surveys were made at the bottom and right side of the annulus for inlets A and B,l inch and 1/8 inch, respectively, downstream of the inlet. Surveys were also made of the pressures at the top and left side of the diffusers after an area expansion of 11.5 percent (stations 12.4 and 11.8 for inlets A and B, respectively). Inlet A had an additional rake located halfway between the other two diffuser rakes. A typical rake may be seen in figure 6.

Pressure surveys were conducted at angles of attack of -6°, 0°, and 6° for ten values of inlet-velocity ratio ranging between 0.25 and 1.65. Pressure surveys for the parts of the model diametrically opposite to the instrumentation were obtained by the expedient of testing at the numerically equal negative angle of attack. A tunnel speed of 100 miles per hour, which corresponds to a Mach number of 0.13 and a Reynolds number of about 2,000,000 based on the maximum cowling diameter, was used for tests at inlet-velocity ratios up to 0.9 for inlet A and up to 1.2 for inlet B. For the remaining tests, the tunnel speed was reduced to about 70 miles per hour in order to obtain the higher inlet-velocity ratios with the available fan power.

## RESULTS AND DISCUSSION

Nose and inner surface of diffuser. Surface pressure distributions over the nose and inner surface of the diffuser of each of the two inlets are presented as figure 7. At an angle of attack of 00, flow velocities over the surfaces ahead of the inlets were

substream at inlet-velocity ratios below unity. As would be expected, the velocities on the nose of inlet B were much lower than those for inlet A because of the greater cone angle. Increasing the angle of attack increased the flow velocities at the upper forward parts of the nose cones and the bottom of the inlets (as indicated by the data for  $\alpha = -6^{\circ}$ ) and reduced the velocities at the tops of the inlets. At the lowest test inlet-velocity ratios, the surface pressure distributions indicate boundary-layer separation from the top surfaces just in front of the inlets for  $\alpha = 6^{\circ}$ .

The surface pressures at the inlets of both configurations at  $\alpha = 0^{\circ}$  (fig. 7) were always more negative than corresponding estimated values based on the inlet-velocity ratio because the inlet-velocity distribution was nonuniform due to the boundary layers on the noses and also because of the curvature of the nose cone near the plane of the inlet. Maximum velocities on the central bodies of both configurations occurred aft of the inlet for all test conditions despite the fact that the minimum duct area occurred at the inlet. This phenomenon can, for the higher inlet-velocity ratios, be partly attributed to a small reduction in the effective area aft of the inlet caused by separation of the flow from the sharp-edge inlet lips; as will appear later, such separation was more pronounced for inlet B than for inlet A for the same inlet-velocity ratio. The effect is also due to the fact that the center of the curved transition region between the cone and the inner wall of the diffuser occurs aft of the inlet, particularly for nose B. In general, velocity tends to be a maximum near the center of a curved transition region between two straight surfaces.

Inlet lips .- Pressure distributions over the lips of the test inlets for  $\alpha = 0^{\circ}$  (fig. 8) show that large negative pressure peaks occurred on the outside surfaces just behind the leading edges at the lower inlet-velocity ratios and on the inside surfaces just behind the leading edges at the higher inlet-velocity ratios; hence, these inlets operate without high pressure peaks only in a narrow range of inlet-velocity ratio. The shapes of the pressure distributions indicate that separation bubbles existed at these points in conjunction with these pressure peaks. The separation bubble on the external surface of inlet B was smaller than that for inlet A because of the greater camber of the lip. At the top of the inlet the effect of increasing the angle of attack was to broaden and increase the magnitude of the external pressure peaks and to decrease the magnitude of the internal pressure peaks; the data for  $\alpha = -6^{\circ}$ (fig. 8(c)) indicate opposite trends existed at the bottoms of the inlets.

Total-pressure surveys in the boundary layer near the rear of the cowlings are presented in figure 9. A plot of the boundary-layer thicknesses corresponding to these data against inlet-velocity ratio (fig. 10) shows that at  $\alpha=0^\circ$  severe separation from the lips of either cowling did not occur above inlet-velocity ratios of about 1.0. Below this inlet-velocity ratio inlet B showed only a slight thickening of the boundary layer whereas inlet A showed rapidly increasing boundary-layer thickness. A comparison of the data in figure 9(a) with comparable data in figure 16 of reference 3 also indicates that for inlet A the boundary layer on the external lip surface is much thicker and therefore the external drag would probably be higher than that for the NACA transonic inlet of references 2 and 3 for most of the useful range of inlet-velocity ratio.

It is noted that at the higher test values of inlet-velocity ratio, the pressure distribution over the external part of the lip of inlet B (fig. 8) was fairly flat as is characteristic of the pressure distributions for the NACA 1-series nose inlets of refer-

ence 4. At  $\alpha = 0^{\circ}$  and  $\frac{v_i}{v_o} = 0.9$ , the critical Mach number for

this surface predicted according to reference 5 was 0.74, a value of the same order as that estimated for the NACA 1-77.5-050 nose inlet which was used as the basic transition shape. This result indicates that the transition fairing aft of the wedge-shape lip section can be designed for any desired critical Mach number up to about 0.9 by use of the existing data for the NACA 1-series nose inlets.

The negative pressure peaks on the internal lip surface of inlet B in general were somewhat higher and broader than those for inlet A for equal inlet velocity ratios. (See fig. 8.) This result indicates that, as previously deduced, the size of the separation bubble on the inside of the lip of such inlets tends to increase as the camber of the lip is increased. However, the flow returned to the surface quickly in both cases. Subsequent results show that the internal separation losses were not excessive for either inlet

up to  $\frac{V_i}{V_O}$  = 1.2, but were larger for inlet B than for inlet A at the higher values of inlet-velocity ratio.

Minimum surface pressures and critical Mach numbers. The minimum surface pressures measured at the top of the model for angles of attack of  $-6^{\circ}$ ,  $0^{\circ}$ , and  $6^{\circ}$  are given in figure 11; corresponding critical Mach numbers predicted according to reference 5 are summarized in figure 12. The data for  $\alpha = -6^{\circ}$  may be regarded as being applicable to the bottom section of the inlets for  $\alpha = 6^{\circ}$ .

The most important item to be noted in figures 11 and 12 is that for angles of attack of both 0° and 6° the velocities on the nose of inlet B remained substream up to an inlet-velocity ratio of the order of 1.1 and were lower than the velocities on the diffuser surfaces just inside the inlet for the higher test values of  $V_i/V_o$ . Accordingly, for subsonic flight speeds it would be expected that the inlet would choke before any local supersonic speed appeared on the cone. The data for inlet A indicate approximately this same conclusion, although the margin of safety is considerably less than for inlet B.

Means for increasing the critical speed of the external lip surfaces were not investigated in the present tests. However, as previously noted, it appears that this might be accomplished by using a higher-critical-speed NACA l-series nose-inlet shape (reference 4) in the transition fairing between the sharp inlet lip and the maximum thickness section of the fuselage.

Pressure surveys in inlets. Pressure surveys at the inlets of the two test configurations are presented in figure 13. At an angle of attack of 0°, the boundary layer on the conical nose of inlet A appeared to be separated at the lowest inlet-velocity ratio and was much thicker than that for inlet B for all test inlet-velocity ratios. The effect of increasing angle of attack was to increase the inlet-velocity ratio at which separation occurred at the top of the inlet and to produce the opposite effect at the bottom. Inlet-velocity ratios of about 0.9 and 0.7 were required at an angle of attack of 6° to avoid separation at the tops of inlets A and B, respectively. The pressure distributions at the sides of the inlets were essentially the same for angles of attack of 0° and 6°.

Pressure surveys in diffusers. Pressure surveys in the diffusers of the two test configurations after an area expansion of 11.5 percent are shown in figure 14. At the lower inlet-velocity ratios, the boundary layers on the inner surface of the diffuser were very thick and composed the major part of the total losses. However, at inlet-velocity ratios above unity, which may be important for the subsonic flight regime, the separation losses from the inner part of the inlet lip became more important than the boundary-layer losses at the inner surface of the diffuser.

The averages, obtained by integration, of the total-pressure recoveries in the diffusers of the two test configurations are presented in figure 15 as functions of the inlet-velocity ratio for angles of attack of 0° and 6°. The pressure recoveries for inlet B were over 90 percent of  $\mathbf{q}_0$  below an inlet-velocity ratio of about unity and were slightly higher than those for inlet A because of the

smaller boundary layer at the inlet. Above an inlet-velocity ratio of about unity the pressure recovery for inlet B was less than that for inlet A because of the more severe separation from the lip of inlet B.

A comparison of the data contained in figure 15 with corresponding pressure recoveries for the NACA transonic air inlet (after 17 percent area expansion, reference 3) shows that the pressure recoveries for the two inlets were of the same order below an inlet-velocity ratio of about 1.2. Above this inlet-velocity ratio much higher pressure recoveries were obtained with the NACA transonic air inlet due to the avoidance of separation from the inner surface of its inlet lip. The NACA transonic inlet would be expected to exhibit a much higher pressure recovery in the climb condition.

## CONCLUDING REMARKS

A wind-tunnel investigation has been made to determine the lowspeed characteristics of two sharp-edge supersonic air inlets designed
for essentially external supersonic compression in accordance with
the investigation of NACA RM No. L6J31. Inlet A, which was designed
for flight Mach numbers up to 1.2, was a configuration similar to
the NACA transonic inlet investigated in the tests of NACA RM No. L6J04
and NACA RM No. L7A06 and therefore provides a comparison between a
sharp-edge and a conventional (subsonic) cowling. Inlet B, which was
designed for supersonic flight Mach numbers up to about 3.0, was representative of the inlet used in the tests of NACA RM No. L6J31. The
results of the investigation are summarized as follows:

- 1. Sharp-edge cowlings of this type will operate without high pressure peaks only in a narrow range of inlet-velocity ratio. Sharp pressure peaks with steep adverse gradients appear outside of this range on the external surface at lower inlet-velocity ratios and on the internal surface at higher inlet-velocity ratios.
- 2. The separation caused by the severe pressure peaks on such sharp-edge cowling lips is at first largely confined to a "bubble" near the leading edge; however, total-pressure losses due to the separation are reasonably low for a fairly wide range of inlet-velocity ratio.
- 3. Internal losses for both inlets tested were of the same order as those measured for the NACA transonic inlet of NACA RM No. L7A06 below an inlet-velocity ratio of 1.2. At inlet-velocity ratios above this value the NACA transonic inlet, with its rounded lip, evinces a higher pressure recovery. Similarly, it is indicated

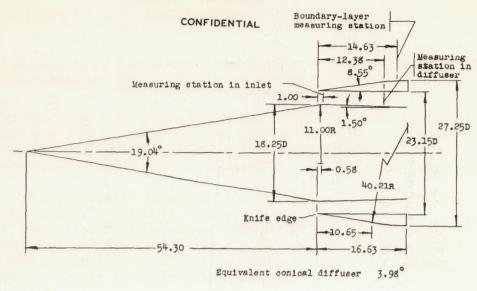
that the external drag for inlets A and B will be higher than that for the NACA transonic inlet, especially at low values of  $V_1/V_0$ .

- 4. For subsonic flight speeds, inlet B would be expected to choke before any local supersonic speed appeared on the nose cone. The data for inlet A indicate approximately this same conclusion, although the margin of safety is considerably less than for inlet B.
- 5. The desirable flat pressure distribution over the external cowling surface may be obtained by using the NACA 1-series nose inlet as a transition fairing between the sharp leading edge and the maximum cowling diameter. It is possible by use of this method to design sharp-edge inlets which will have critical Mach numbers up to about 0.9 in the subsonic flight regime.

Langley Memorial Aeronautical Laboratory
National Advisory Committee for Aeronautics
Langley Field, Va.

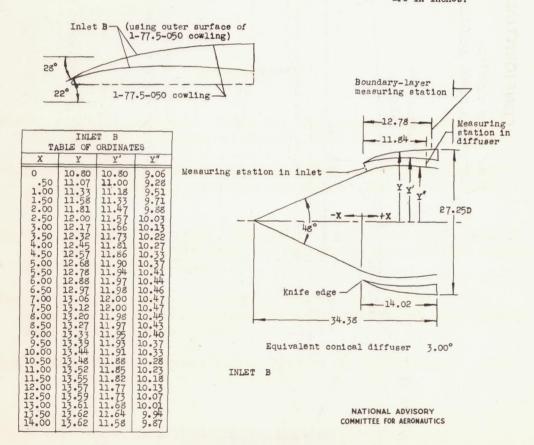
#### REFERENCES

- 1. Ferri, Antonio, and Nucci, Louis M.: Preliminary Investigation of a New Type of Supersonic Inlet. NACA RM No. L6J31, 1946.
- Nichols, Mark R., and Rinkoski, Donald W.: A Low-Speed Investigation of an Annular Transonic Air Inlet. NACA RM No. L6J04, 1946.
- 3. Nichols, Mark R., and Goral, Edwin B.: A Low-Speed Investigation of a Fuselage-Side Air Inlet for Use at Transonic Flight Speeds. NACA RM No. 17A06, 1947.
- 4. Baals, Donald D., Smith, Norman F., and Wright, John B.: The Development and Application of High-Critical-Speed Nose Inlets. NACA ACR No. L5F30a, 1945.
- 5. von Karmán, Th.: Compressibility Effects in Aerodynamics. Jour. Aero. Sci., vol. 8, no. 9, July 1941, pp. 337-356.



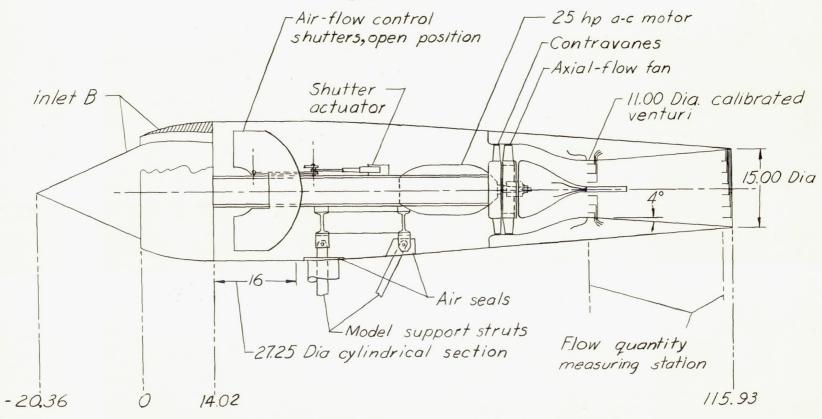
INLET A

Note: All dimensions are in inches.



CONFIDENTIAL

Figure 1.- Arrangement and dimensions of nose sections of model.



Note: All dimensions are in inches

NATIONAL ADVISORY
COMMITTEE FOR AERONAUTICS

Figure 2. - Arrangement and overall dimensions of model.

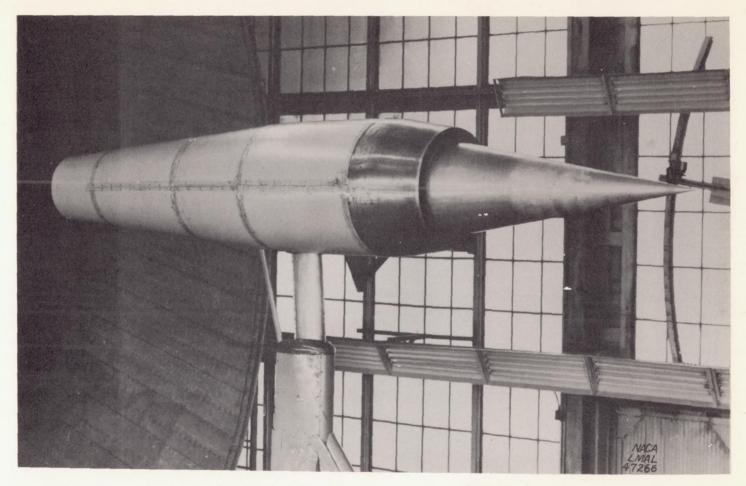


Figure 3.- General view of model mounted in propeller-research tunnel; Inlet A. CONFIDENTIAL

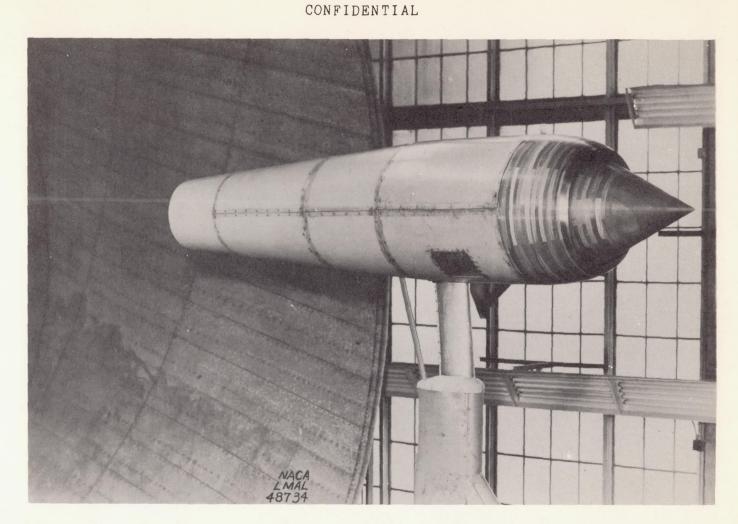


Figure 4.- General view of model mounted in propeller-research tunnel; Inlet B.



Figure 5.- Detail view of Inlet A.

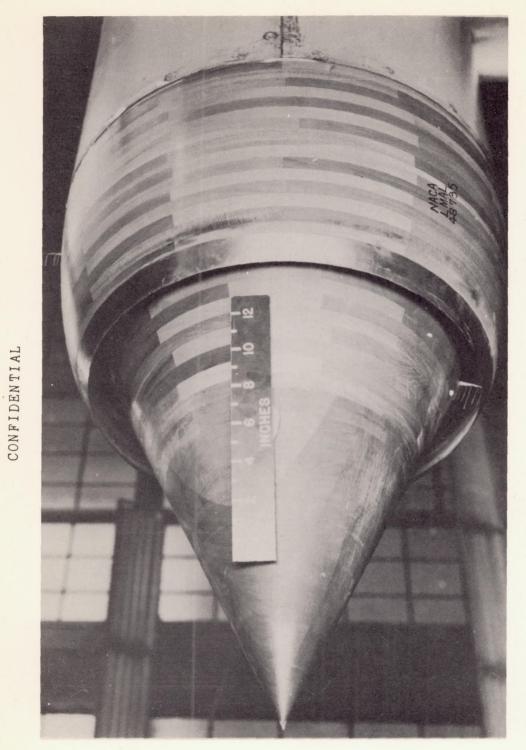


Figure 6.- Detail view of Inlet B.

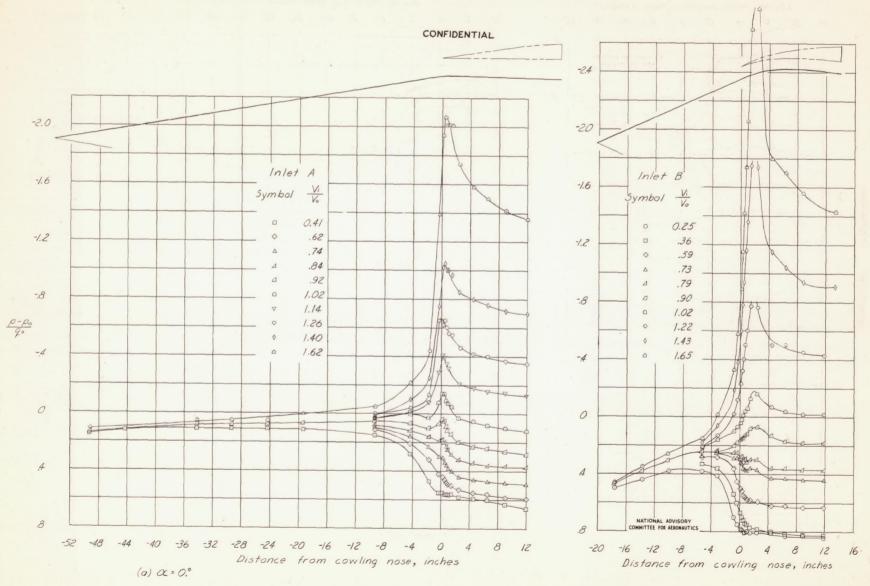


Figure 7 .- Static pressure distributions over nose and inner surface of diffuser at top of model.

CONFIDENTIAL

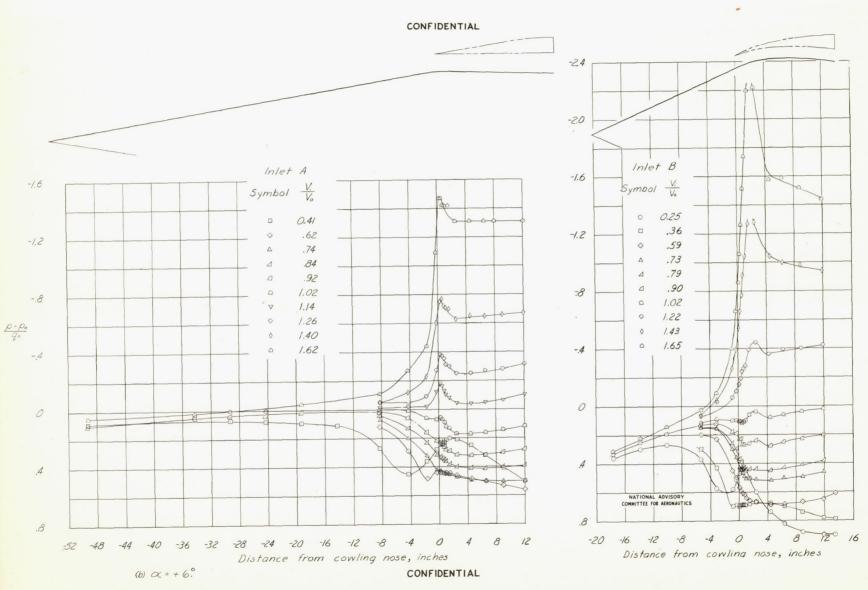
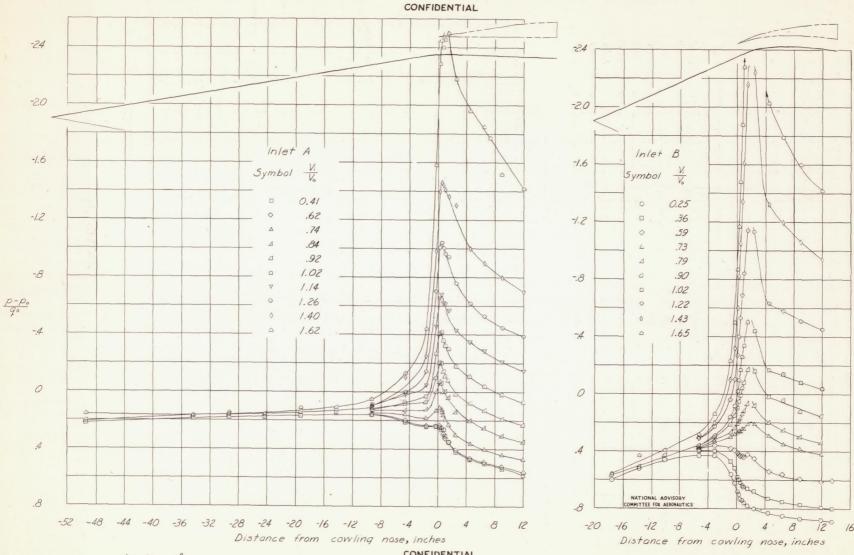


Figure 7 .- Continued.



(c) a=-6° Figure 7 .- Concluded.

CONFIDENTIAL

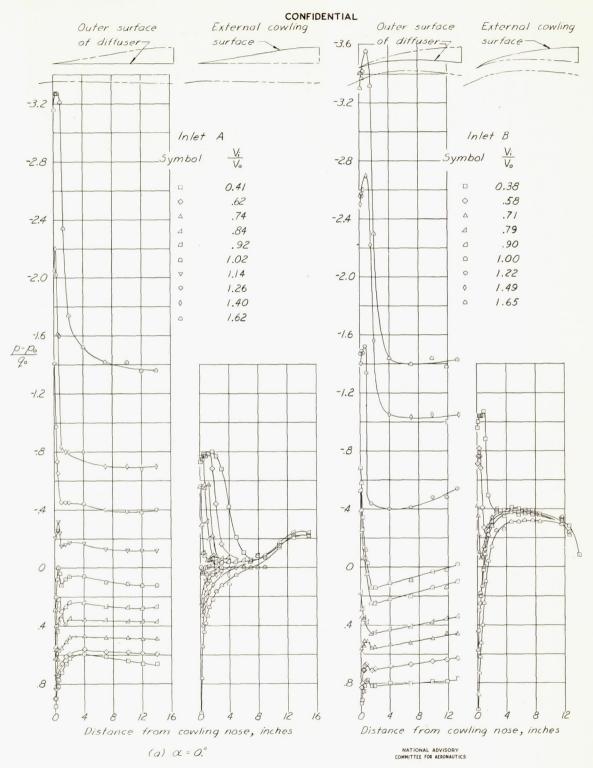


Figure 8 .- Static pressure distributions at top section of inlet lip.

CONFIDENTIAL

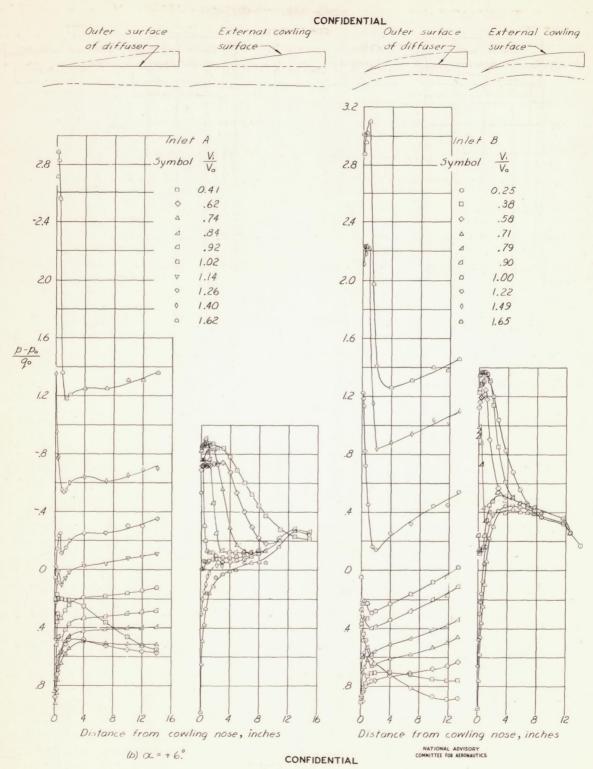


Figure 8 .- Continued.

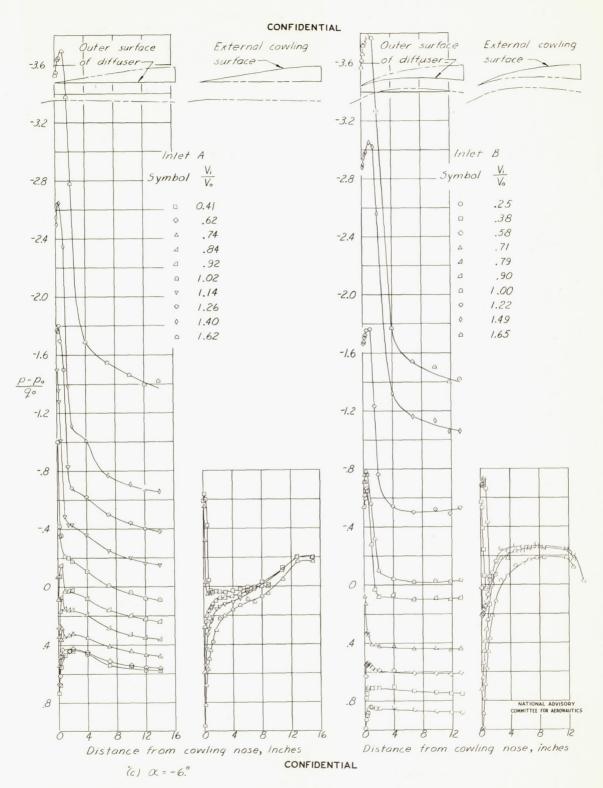


Figure 8 .- Concluded.

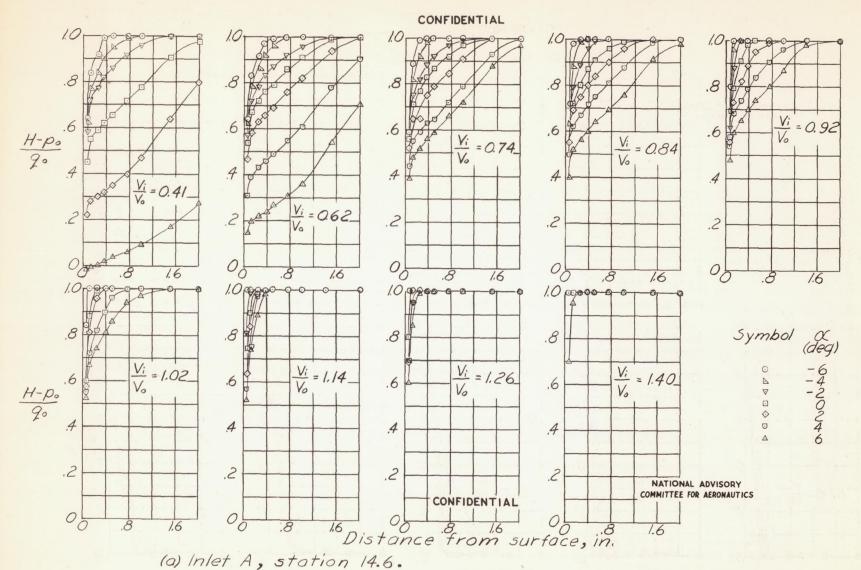
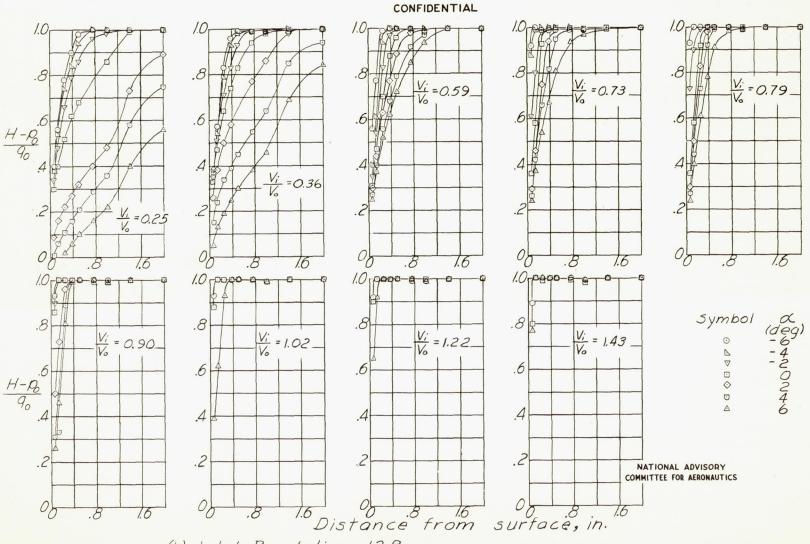
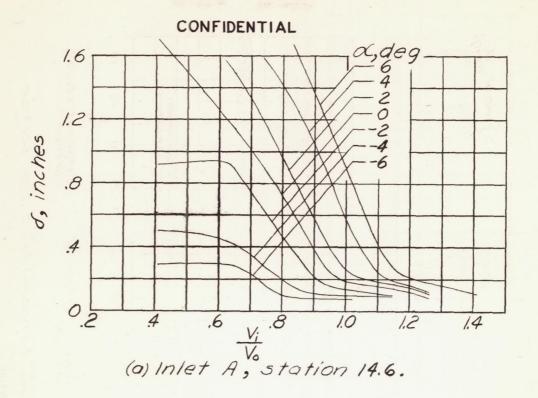


Figure 9.- Total pressure distribution in external flow at top of cowling.



(b) Inlet B, station 12.8. CONFIDENTIAL Figure 9 . - Concluded.



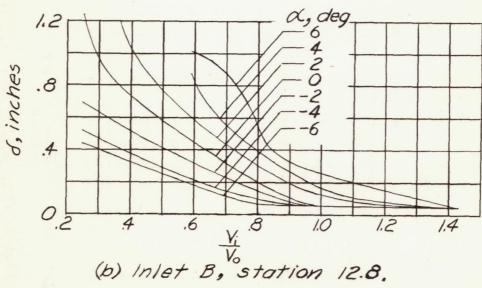


Figure 10. - Boundary layer thickness on top of cowlings. NATIONAL ADVISORY

COMMITTEE FOR AERONAUTICS

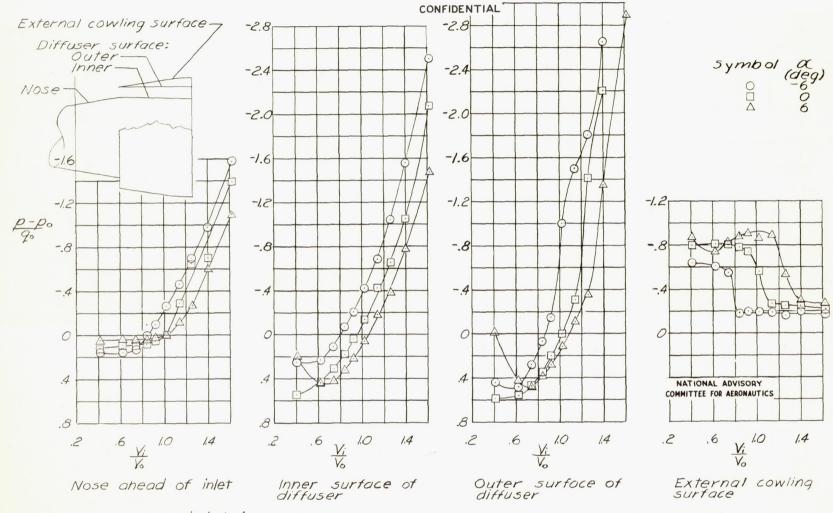
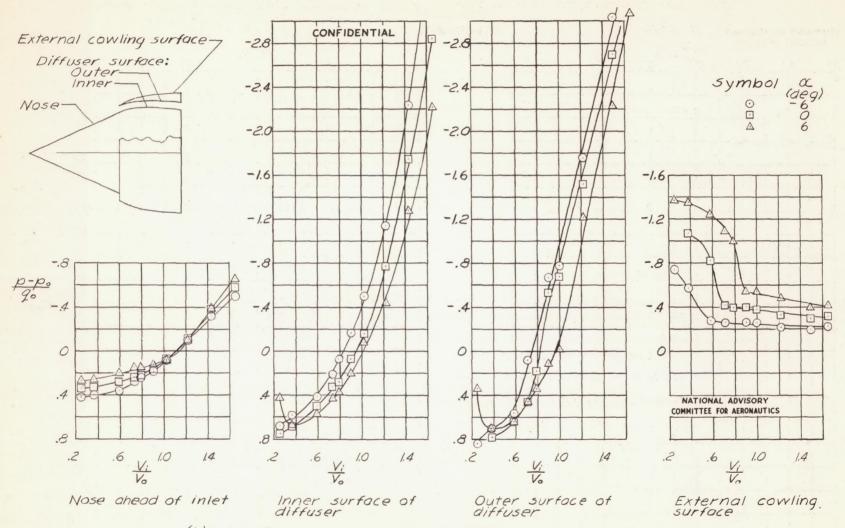


Figure 11.- Minimum pressures on model components at top portion of model. CONFIDENTIAL



(b) Inlet B. Figure 11. - Concluded.

CONFIDENTIAL

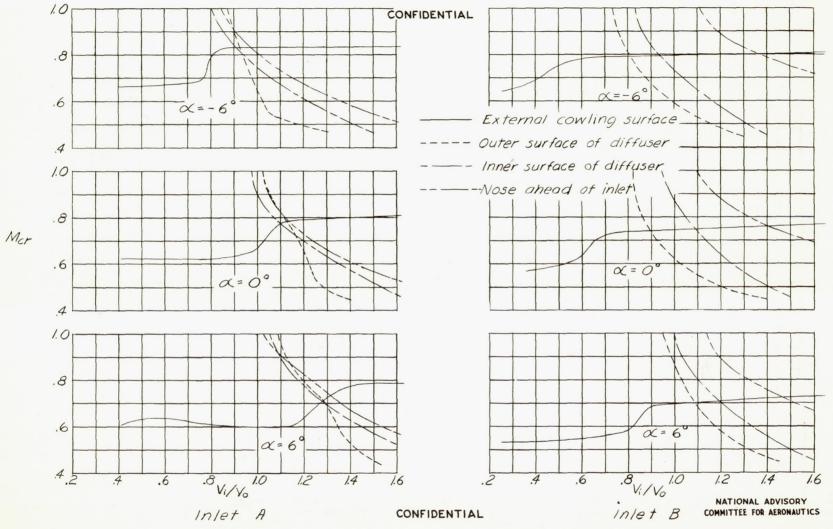


Figure 12. - Predicted critical Mach number characteristics of top portion of model,

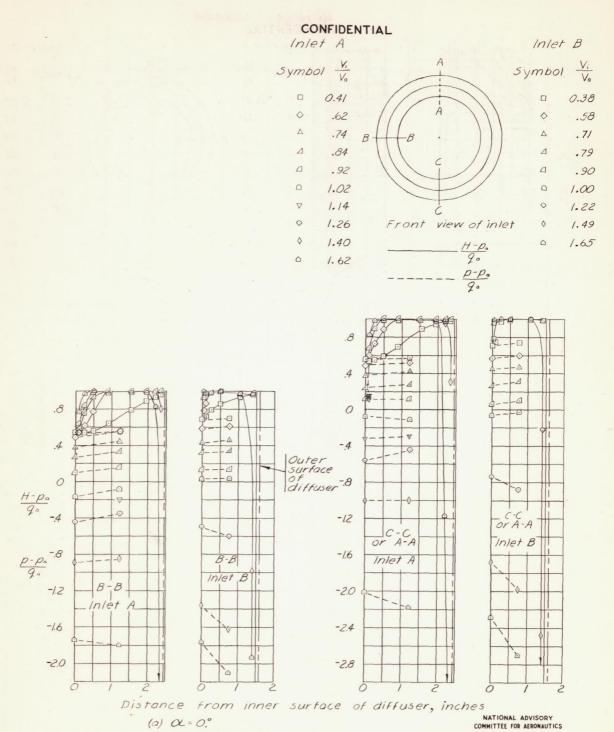


Figure 13. - Pressure surveys at measuring stations in inlets.

CONFIDENTIAL

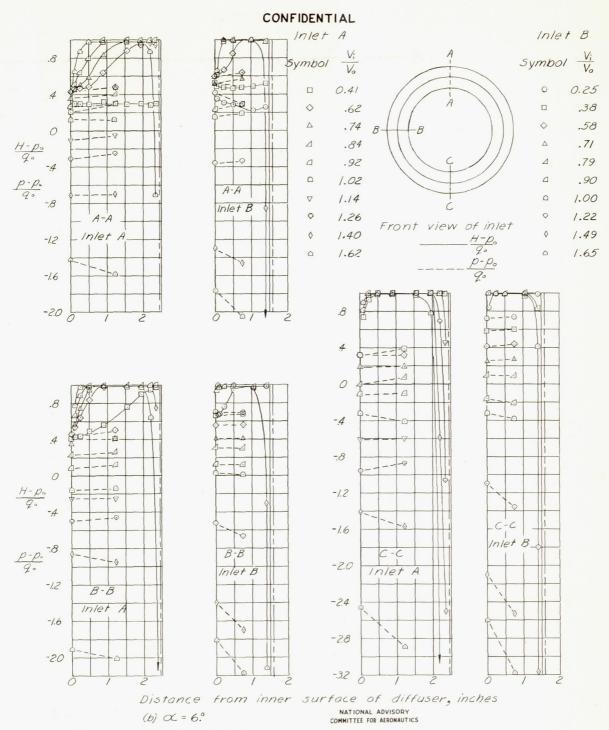
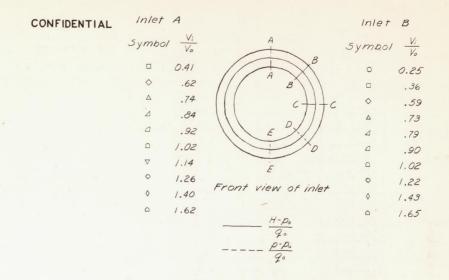


Figure 13 . - Concluded.

CONFIDENTIAL



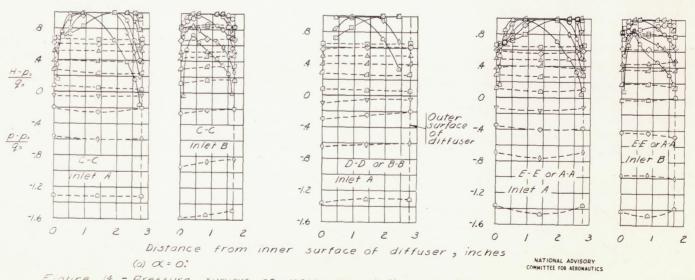


Figure 14. - Pressure surveys at measuring stations in diffusers.

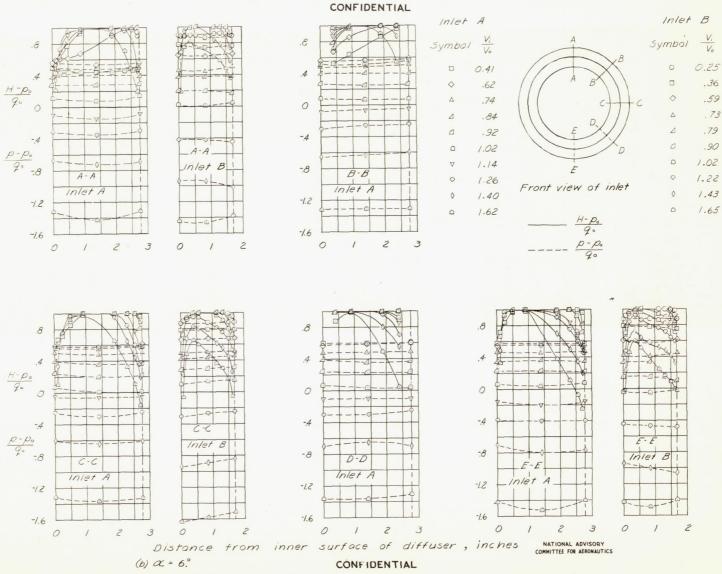


Figure 14. - Concluded.

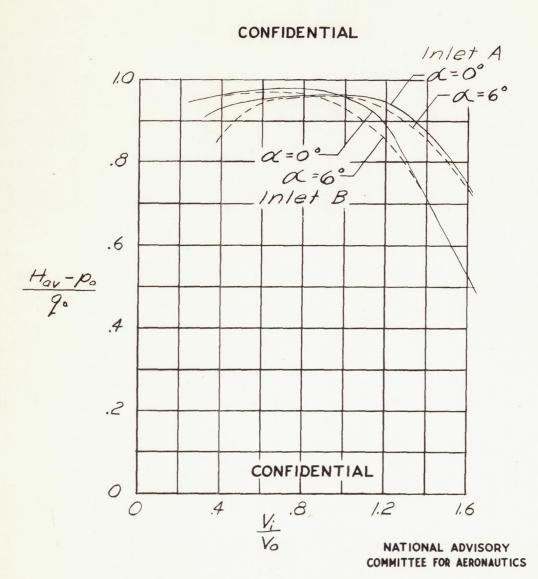


Figure 15. - Average total-pressure recovery at measuring stations in diffusers.